



ELSEVIER

Contents lists available at SciVerse ScienceDirect

Biosensors and Bioelectronics

journal homepage: www.elsevier.com/locate/bios

Short communication

Highly sensitive, label-free colorimetric assay of trypsin using silver nanoparticles

Peng Miao^{a,b}, Tao Liu^a, Xiaoxi Li^b, Limin Ning^b, Jian Yin^a, Kun Han^{a,*}^a Department of Medical Diagnostics, Suzhou Institute of Biomedical Engineering and Technology, Chinese Academy of Sciences, Suzhou 215163, PR China^b Department of Biochemistry and National Key Laboratory of Pharmaceutical Biotechnology, Nanjing University, Nanjing 210093, PR China

ARTICLE INFO

Article history:

Received 14 February 2013

Received in revised form

10 April 2013

Accepted 24 April 2013

Available online 3 May 2013

Keywords:

Silver nanoparticles

Trypsin

Biosensor

Label-free

ABSTRACT

Herein, we report a simple, sensitive label-free colorimetric assay of trypsin based on silver nanoparticles (AgNPs) aggregation. Generally, a specially designed short peptide chain acts as both the stabilizer of AgNPs and the substrate of trypsin. In the presence of trypsin, the negatively charged part of peptides will be hydrolyzed, leaving the positively charged dipeptide capped on the surface of AgNPs. The electrostatic property alteration then leads to the AgNPs' aggregation in certain salt condition. The solution color may change correspondingly due to the localized surface plasmon resonance, which can be monitored by naked eye and UV–vis spectrophotometry. This novel AgNPs-based colorimetric method for quantitative determination of trypsin has a linear detection range from 2.5 to 200 ng mL⁻¹ and a rather low detection limit down to 2 ng mL⁻¹. The determination of trypsin can also be realized in complex biological fluids by the proposed method, demonstrating its great potential utility in the clinical applications in the future.

© 2013 Elsevier B.V. All rights reserved.

1. Introduction

Trypsin is a kind of serine protease produced in the pancreas that cleaves proteins on the C-terminal side of arginine or lysine residues. The initial proenzyme form of trypsinogen can self-cleave to generate the active form of trypsin, which then induces the transformation of other pancreatic proenzymes into the active forms. Therefore, trypsin plays a critical role in the control of pancreatic exocrine function (Hirota et al., 2006; Rawlings and Barrett, 1994). The level of trypsin can serve as a reliable and specific diagnostic biomarker for pancreatic function and its pathological changes such as pancreatitis, cystic fibrosis and cancer (Artigas et al., 1981; Byrne et al., 2002). For example, the serum trypsin concentration of acute pancreatitis patients is much higher than that of healthy individuals. Moreover, trypsin has been widely employed in food industry and biotechnology applications (Schuchert-Shi and Hauser, 2009; Soleimani and Nadri, 2009), thus developing simple, selective and sensitive methods for the detection of trypsin which has attracted increasing attention.

Traditional methods for quantifying trypsin usually involve radioimmunoassay (Temler and Felber, 1976), gelatin-based film assay (Kersey et al., 1993) and enzyme-linked immunosorbent assay (Rhodes et al., 1957). So far, a large number of biosensors have been developed, such as electrochemical (Ionescu et al.,

2006; Stoytcheva et al., 2012; Wang et al., 2012b), fluorescent (An et al., 2009; McKenzie et al., 2009; Wang et al., 2010a, 2010b), colorimetric (Xue et al., 2011) and Quartz Crystal Microbalance (QCM) (Stoytcheva et al., 2013) sensors. However, these methods require either sophisticated and expensive equipment, or time-consuming and laborious experiment procedures like molecule labeling, which can be operated only by well-trained professionals. Hence, simple, fast and precise methods to quantify trypsin should be developed for rapid clinical applications. Recently, Zaccheo and Crooks have fabricated a delicate self-powered sensor for trypsin using light-emitting diode (LED) to deliver a visible response (Zaccheo and Crooks, 2011). Nevertheless, the sensitivity of this device is not satisfactory and the assay time is about 3 h, which is too long.

Colorimetric biosensors based on gold nanoparticles (AuNPs) and silver nanoparticles (AgNPs) are now gaining more and more attention due to the advantages such as simplicity, fast response, cost-effectiveness and high sensitivity (Ravindran et al., 2011; Su et al., 2011; Wang et al., 2006, 2012a). Moreover, AgNPs have certain merits over AuNPs since they possess higher extinction coefficients comparing with AuNPs of the same size (Lee et al., 2007). Herein, we report a novel label-free colorimetric method for quantifying trypsin using AgNPs. In this work, a short peptide substrate has been designed to cap AgNPs for stabilization via silver–sulfur interaction (Taglietti et al., 2012). Trypsin can cleave the C-terminal side of arginine in this peptide, which leads to the release of the negatively charged peptide chain into the solution and the positively charged dipeptides remaining on the surface of

* Corresponding author. Tel./fax: +86 512 69588230.

E-mail address: hank@sibet.ac.cn (K. Han).

AgNPs. The variation of the electrostatic property then triggers the aggregation of AgNPs. Since the aggregation is strongly correlated with the remarkable property known as localized surface plasmon resonance (LSPR) (Sherry et al., 2005), the distribution state of AgNPs altered by trypsin can be observed by a common spectrophotometer or even by the naked eye. The assay time is short and the limit of detection (LOD) can be as low as 2 ng mL^{-1} , which promises the method great potential utility for point-of-care test (POCT).

2. Experimental

2.1. Materials and chemicals

Peptide (Cys–Arg–Ala–Asp–Asp–Asp, CRADDD) was synthesized and purified by Chinapeptides Co., Ltd. Silver nitrate (AgNO_3), trisodium citrate, sodium borohydride (NaBH_4), trypsin, glucose oxidase (GOx), thrombin, alkaline phosphatase (ALP), lysozyme and Bowman-Birk inhibitor (BBI) were purchased from Sigma-Aldrich. Human serum samples were supplied by the local hospital and human urine samples were collected from healthy volunteers. The other reagents were of analytical grade and used as received. All solutions were prepared with double-distilled water, which was purified with a Milli-Q purification system (Branstead, USA) to a specific resistance of $18 \text{ M}\Omega \text{ cm}$.

2.2. Apparatus

UV absorption spectra were recorded by a Synergy HT multi-function microplate reader (BioTek Instruments, Inc., USA). Transmission electron micrographs were taken using FEI Tecnai G20 transmission electron microscope (TEM) (FEI company, USA). Photographs were taken with a Canon IXUS220 HS digital camera.

2.3. Preparation of peptide-capped AgNPs

AgNPs were synthesized by borohydride reduction of AgNO_3 as reported previously (Doty et al., 2005). Briefly, the solution of 0.25 mM AgNO_3 and 0.25 mM trisodium citrate was prepared. Then, 3 mL aqueous solution of NaBH_4 (10 mM) was added to 100 mL of the mixture of AgNO_3 and trisodium citrate under vigorous stirring during a period of 30 min . The formed AgNPs were left to sit for 24 h . After that, the AgNPs were purified by three cycles of centrifugation at $12,000\text{g}$ for 20 min and the pH value was finally adjusted to 8.0 using phosphate buffered saline (PBS, 2 mM). The functionalization of AgNPs with the peptide was achieved by the silver–sulfur chemistry. After 24 h incubation, the excess peptides were removed by centrifuging at $12,000\text{g}$ for 20 min .

2.4. Experimental conditions optimization

To obtain the optimal experimental conditions, several parameters were examined, including the incubation time and the concentrations of NaCl and peptides.

2.4.1. The concentration of NaCl

Freshly prepared AgNPs could keep stable for several months. Nevertheless, if certain amount of salt was added into AgNPs, aggregation might occur and the solution color might change accordingly. Solutions with various NaCl concentrations ranging from 0 to 0.1 M were prepared and mixed with AgNPs. UV absorption spectra were measured from 300 nm to 700 nm and the ratios of net decreased absorbance peak ($\Delta A/A_0$) were

calculated. A critical value of NaCl concentration was then chosen to represent the salt-tolerance of AgNPs.

2.4.2. The concentration of peptide

Solutions with various peptide concentrations were firstly added to AgNPs solutions separately. After 24 h incubation, the excess peptide was removed by centrifugation at $12,000\text{g}$ for 20 min . The salt-tolerance of the peptide-capped AgNPs was examined by adjusting the NaCl concentration to the critical value.

2.4.3. Incubation time

The optimal incubation time of peptide-capped AgNPs and NaCl was determined by monitoring UV absorption spectra after mixing them for different time durations.

2.5. UV-vis spectroscopy analysis of trypsin

The optical detection of trypsin was carried out as follows. 0.2 M peptide was used to cap AgNPs. The prepared nanoparticles were then treated by trypsin with various concentrations ranging from 0 to 500 ng mL^{-1} at 37°C for a period of 10 min . Subsequently, the UV-vis absorption spectra were measured to check the salt-tolerances of the solutions with 0.036 M NaCl.

2.6. Inhibition and interference of trypsin in the assay

The proposed method was further used to evaluate the inhibition of trypsin by BBI (Rawlings et al., 2004). $5 \mu\text{g mL}^{-1}$ BBI was introduced to inhibit the activity of trypsin (100 ng mL^{-1}) in peptide-capped AgNPs solutions.

Moreover, to examine the specificity and selectivity of this method, some interfering proteins such as GOx, thrombin, ALP and lysozyme were employed as control to replace trypsin in the detection system.

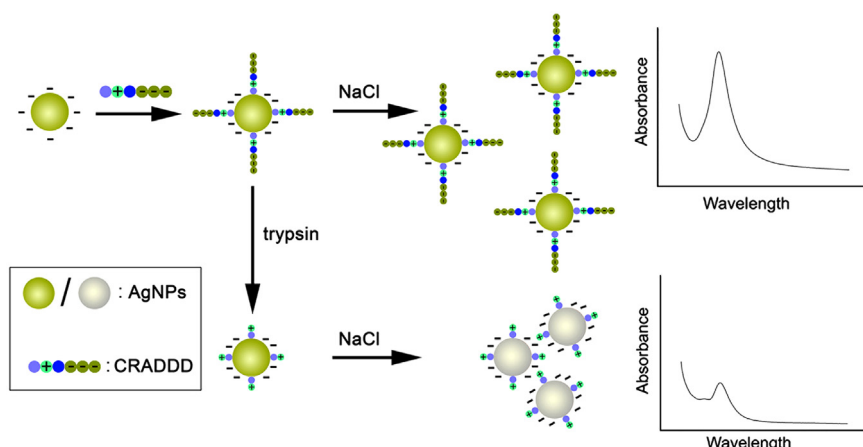
2.7. Determination of trypsin in serum and urine samples

To verify the utility of this method in complex biological fluids, human serum and urine samples were introduced. Since dilution is a commonly used pretreatment procedure for protein analysis in samples with high complexity, both human serum and urine samples were diluted 10 times before the detection of trypsin using the proposed method.

3. Results and discussion

3.1. Sensing principle

The strategy of trypsin assay is illustrated in Scheme 1. A short peptide, CRADDD, is firstly attached to the surface of AgNPs by the sulfhydryl group on the N-terminal amino acid via the silver–sulfur interaction. The peptide is negatively charged at appropriate pH, thus it can help stabilize AgNPs and contribute to a significant improvement in salt-tolerant performance of AgNPs. However, if the test solution contains certain amount of trypsin, CRADDD on AgNPs can be easily hydrolyzed. Then, a shorter negatively charged peptide, ADDD, is released while the positively charged CR sticks on the surface of AgNPs. As a result, the negative charge density on AgNPs surface decreases and the electrostatic stability is broken, which may lead to the aggregation of AgNPs. The resulted color change can then be used to reflect the concentration of trypsin in the test solution. Moreover, the hydrolysis of CRADDD by trypsin can be retarded in the presence of inhibitors, and the aggregation of AgNPs can thereby be prevented.



Scheme 1. Schematic representation of the colorimetric assay of trypsin.

3.2. Characterization of AgNPs

The synthesis of AgNPs involves the reduction of Ag^+ by NaBH_4 with trisodium citrate. The color of final AgNPs suspension is yellow and transparent, demonstrating the good dispersion in water. The diameter of around 5 nm is determined by TEM image (Fig. S1A). Moreover, the UV-vis spectrum of AgNPs displays the characteristic absorbance peak at the wavelength of 394 nm due to the surface plasmon excitation (Fig. S1B).

3.3. Preliminary experiments

Preliminary experiments have been carried out to determine the optimal experiment conditions for trypsin assay.

The absorbance peak of peptide-capped AgNPs is at the wavelength of 394 nm. With more NaCl in the solution, the absorbance peak appears smaller (Fig. 1A). $\Delta A/A_0$ is employed to reveal the distribution state of AgNPs. The relationship between $\Delta A/A_0$ and the concentration of NaCl is displayed in Fig. 1B. The fitting curve is a Boltzmann sigmoid with the equation of

$$y = A_2 + (A_1 - A_2) / (1 + \exp((x - x_0) / dx)) \quad (A_1 = 0.00074, \quad A_2 = 0.83897, \quad x_0 = 0.036, \quad dx = 0.00628, \quad R^2 = 0.99126).$$

Obviously, when the concentration of NaCl equals to 0.036 M, the slope of this curve reaches the maximum value, indicating that this solution is most sensitive to the changes of NaCl concentration at this critical point. Therefore, this value is adopted to evaluate the effects of peptide stabilization and trypsin hydrolysis in further investigation.

In the experiment to obtain the optimal peptide concentration, different amounts of peptide is incubated with AgNPs before the experiments to check the salt-tolerance of 0.036 M NaCl. Experiment results show that the parameter of $\Delta A/A_0$ reaches a saturation value when the peptide concentration is 0.2 μM (Fig. S2). Thus, this concentration is applied in further experiments to stabilize AgNPs.

In these UV-vis spectroscopy experiments, the aggregation of AgNPs reaches a plateau within 10 min. Therefore, 10 min is used as the optimal incubation time.

3.4. UV-vis spectroscopy analysis of trypsin by peptide-capped AgNPs

A series of concentrations of trypsin are used to incubate with peptide-capped AgNPs. The spectra information is used for the analysis of the concentration of trypsin, which can be visualized by the naked eye (Fig. 1C). The results show that with the increase of trypsin, more CRADDD is hydrolyzed, leading to less electrostatic

stability and weaker salt-tolerance of AgNPs. The AgNPs aggregates more drastically and the absorbance peak is getting smaller. We also take TEM image to monitor the aggregation state of AgNPs after the treatment with 200 ng mL^{-1} trypsin (Fig. S3). Moreover, the size distributions of the peptide-capped AgNPs treated by trypsin have been analyzed by dynamic light scattering (DLS) characterization, showing that almost all particles are larger than 100 nm (Fig. S4).

Fig. 1D shows the calibration curve reflecting the relationship between $\Delta A/A_0$ and trypsin concentration. The inset in Fig. 1D reveals that $\Delta A/A_0$ is linearly dependent on the trypsin concentration in the range of 2.5–200 ng mL^{-1} . The fitting equation is $y = 0.01194 + 0.00341x$ ($n = 4, R^2 = 0.99523$), where y is $\Delta A/A_0$ and x is the concentration of trypsin. The LOD is calculated to be 2 ng mL^{-1} ($S/N = 3$), which is rather low. The average coefficient of variation is 5.93%, demonstrating that the precision of the proposed method is acceptable.

Moreover, we have compared this method with some other reported detection methods (Table S1). Compared with these well-known methods, the proposed sensing strategy has comparable sensitivity to the best results, with advantages in operational convenience and the cost-effectiveness.

3.5. Interference and inhibition study

The selectivity of this method to detect trypsin can be evaluated by introducing various interfering proteins in the detection system, including GOx, thrombin, ALP and lysozyme. Although the concentrations of these interferents are high, none of them can cause the hydrolysis of peptide and the corresponding aggregation of AgNPs with large $\Delta A/A_0$ value (Fig. S5).

The inhibition of trypsin by BBI is also studied. With the presence of BBI to inactivate trypsin, the $\Delta A/A_0$ value is significantly decreased and the AgNPs does not aggregate, demonstrating that the coagulation of AgNPs is attributed to the hydrolysis of peptide by trypsin and this process can be retarded by BBI (Fig. S5).

3.6. Determination of trypsin concentration in human serum and urine samples

We have then performed this sensing strategy in human serum and urine samples to further check its accuracy, reliability and selectivity. The results are listed in Table 1. Certain amount of trypsin has been added in the samples and the final concentration of trypsin is calculated according to the obtained spectra information and the regression equation of the standard curve. The

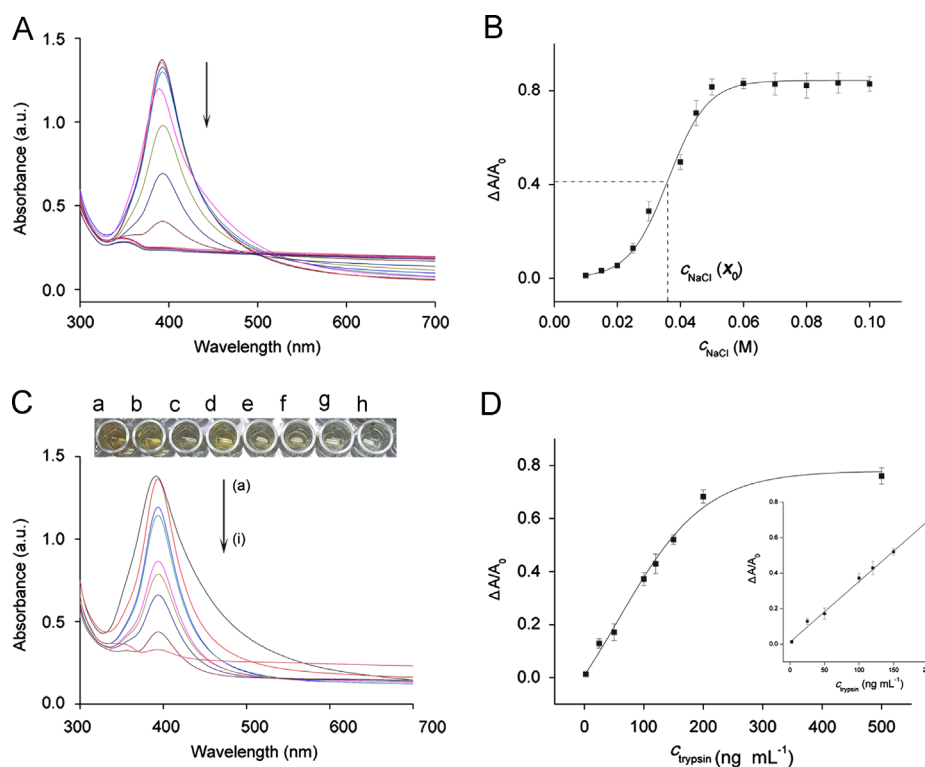


Fig. 1. (A) UV-vis spectra of AgNPs incubated with 0, 0.01, 0.015, 0.02, 0.025, 0.03, 0.04, 0.045, 0.05, 0.06, 0.07, 0.08, 0.09, and 0.1 M NaCl (from top to bottom). (B) $\Delta A/A_0$ of AgNPs versus the concentration of NaCl. The slim dash lines represent the position of the critical point for salt-tolerance. Error bars represent standard deviations of measurements ($n=4$). (C) UV-vis spectra and corresponding solution colors of peptide-capped AgNPs treated with (a) 0, (b) 2.5, (c) 20, (d) 50, (e) 100, (f) 120, (g) 150, (h) 200, and (i) 500 ng mL^{-1} trypsin in the presence of 0.036 M NaCl. (D) Calibration curve of trypsin with a series of concentrations. Inset shows a linear relationship between $\Delta A/A_0$ and the concentration of trypsin. Error bars represent standard deviations of measurements ($n=4$).

Table 1

Results of trypsin assay in adult human serum and urine samples.

Samples	Added (ng mL^{-1})	Detected (ng mL^{-1})	Recovery (%)	Relative error (%; $n=3$)
Serum	50	60.6	121.2	1.22
	100	107.6	107.6	1.35
Urine	50	47.8	95.6	1.03
	100	92.8	92.8	1.15

recoveries and the relative errors summarized in Table 1 confirm satisfactory accuracy and precision of the proposed method. This method may have great potential applications for trypsin assay in clinical diagnosis.

4. Conclusions

In summary, we have fabricated a novel label-free colorimetric method for the determination of trypsin. It is designed based on the aggregation of AgNPs induced by the hydrolysis of CRADD triggered by trypsin. This proposed method has high sensitivity and can be directly applied to human serum and urine samples, demonstrating the resiliency of this method to endogenous interferents in real biological fluids. This biosensor also has the advantages of fast response, low cost and high specificity. Therefore, it has potential use in high-throughput detection of trypsin and may have great potential utility in the clinical applications like pancreatitis diagnosis.

Acknowledgments

This work is supported by the Knowledge Innovative Program of the Chinese Academy of Sciences (KGCX2-YW-913-3).

Appendix A. Supporting information

Supplementary data associated with this article can be found in the online version at <http://dx.doi.org/10.1016/j.bios.2013.04.038>.

References

- An, L.L., Liu, L.B., Wang, S., 2009. *Biomacromolecules* 10 (2), 454–457.
- Artigas, J.M.G., Faure, M.R.A., Garcia, M.E., Gimeno, A.M.B., 1981. *Postgraduate Medical Journal* 57 (666), 219–222.
- Byrne, M.F., Mitchell, R.M., Stiffler, H., Jowell, P.S., Branch, M.S., Pappas, T.N., Tyler, D., Baillie, J., 2002. *Canadian Journal of Gastroenterology* 16 (12), 849–854.
- Doty, R.C., Tshikhudo, T.R., Brust, M., Fernig, D.G., 2005. *Chemistry of Materials* 17 (18), 4630–4635.
- Hirota, M., Ohmuraya, M., Baba, H., 2006. *Journal of Gastroenterology* 41 (9), 832–836.
- Ionescu, R.E., Cosnier, S., Marks, R.S., 2006. *Analytical Chemistry* 78 (18), 6327–6331.
- Kersey, A.D., Berkoff, T.A., Morey, W.W., 1993. *Optics Letters* 18 (16), 1370–1372.
- Lee, J.S., Lytton-Jean, A.K.R., Hurst, S.J., Mirkin, C.A., 2007. *Nano Letters* 7 (7), 2112–2115.
- McKenzie, F., Steven, V., Ingram, A., Graham, D., 2009. *Chemical Communications* 20, 2872–2874.
- Ravindran, A., Mani, V., Chandrasekaran, N., Mukherjee, A., 2011. *Talanta* 85 (1), 533–540.
- Rawlings, N.D., Barrett, A.J., 1994. *Methods in Enzymology* 244, 19–61.
- Rawlings, N.D., Tolle, D.P., Barrett, A.J., 2004. *Biochemical Journal* 378, 705–716.
- Rhodes, M.B., Hill, R.M., Feeney, R.E., 1957. *Analytical Chemistry* 29 (3), 376–378.
- Schuchert-Shi, A., Hauser, P.C., 2009. *Analytical Biochemistry* 387 (2), 202–207.

- Sherry, L.J., Chang, S.H., Schatz, G.C., Van Duyne, R.P., Wiley, B.J., Xia, Y.N., 2005. *Nano Letters* 5 (10), 2034–2038.
- Soleimani, M., Nadri, S., 2009. *Nature Protocols* 4 (1), 102–106.
- Stoytcheva, M., Zlatev, R., Cosnier, S., Arredondo, M., 2012. *Electrochimica Acta* 76, 43–47.
- Stoytcheva, M., Zlatev, R., Cosnier, S., Arredondo, M., Valdez, B., 2013. *Biosensors & Bioelectronics* 41, 862–866.
- Su, H.C., Fan, H., Ai, S.Y., Wu, N., Fan, H.M., Bian, P.C., Liu, J.C., 2011. *Talanta* 85 (3), 1338–1343.
- Taglietti, A., Fernandez, Y.A.D., Amato, E., Cucca, L., Dacarro, G., Grisoli, P., Necchi, V., Pallavicini, P., Pasotti, L., Patrini, M., 2012. *Langmuir* 28 (21), 8140–8148.
- Temler, R.S., Felber, J.P., 1976. *Biochimica et Biophysica Acta* 445 (3), 720–728.
- Wang, L.H., Liu, X.F., Hu, X.F., Song, S.P., Fan, C.H., 2006. *Chemical Communications* 36, 3780–3782.
- Wang, X.H., Geng, J., Miyoshi, D., Ren, J.S., Sugimoto, N., Qu, X.G., 2010a. *Biosensors & Bioelectronics* 26 (2), 743–747.
- Wang, Y.Y., Zhang, Y., Liu, B., 2010b. *Analytical Chemistry* 82 (20), 8604–8610.
- Wang, G.L., Zhu, X.Y., Jiao, H.J., Dong, Y.M., Li, Z.J., 2012a. *Biosensors & Bioelectronics* 31 (1), 337–342.
- Wang, X.W., Wang, Q., Qin, W., 2012b. *Biosensors & Bioelectronics* 38 (1), 145–150.
- Xue, W.X., Zhang, G.X., Zhang, D.Q., 2011. *Analyst* 136 (15), 3136–3141.
- Zaccheo, B.A., Crooks, R.M., 2011. *Analytical Chemistry* 83 (4), 1185–1188.